

# *The role of the cloud radiative effect in the sensitivity of the Intertropical Convergence Zone to convective mixing*

Article

Published Version

Creative Commons: Attribution 4.0 (CC-BY)

Open Access

Talib, J., Woolnough, S. J. ORCID: <https://orcid.org/0000-0003-0500-8514>, Klingaman, N. P. ORCID: <https://orcid.org/0000-0002-2927-9303> and Holloway, C. E. ORCID: <https://orcid.org/0000-0001-9903-8989> (2018) The role of the cloud radiative effect in the sensitivity of the Intertropical Convergence Zone to convective mixing. *Journal of Climate*, 31 (17). pp. 6821-6838. ISSN 1520-0442 doi: <https://doi.org/10.1175/JCLI-D-17-0794.1> Available at <https://centaur.reading.ac.uk/77363/>

It is advisable to refer to the publisher's version if you intend to cite from the work. See [Guidance on citing](#).

To link to this article DOI: <http://dx.doi.org/10.1175/JCLI-D-17-0794.1>

Publisher: American Meteorological Society

All outputs in CentAUR are protected by Intellectual Property Rights law, including copyright law. Copyright and IPR is retained by the creators or other copyright holders. Terms and conditions for use of this material are defined in the [End User Agreement](#).

[www.reading.ac.uk/centaur](http://www.reading.ac.uk/centaur)

**CentAUR**

Central Archive at the University of Reading

Reading's research outputs online

# The Role of the Cloud Radiative Effect in the Sensitivity of the Intertropical Convergence Zone to Convective Mixing

JOSHUA TALIB

*Department of Meteorology, University of Reading, Reading, United Kingdom*

STEVEN J. WOOLNOUGH AND NICHOLAS P. KLINGAMAN

*National Centre for Atmospheric Science–Climate, and Department of Meteorology, University of Reading, Reading, United Kingdom*

CHRISTOPHER E. HOLLOWAY

*Department of Meteorology, University of Reading, Reading, United Kingdom*

(Manuscript received 20 November 2017, in final form 18 May 2018)

## ABSTRACT


Studies have shown that the location and structure of the simulated intertropical convergence zone (ITCZ) is sensitive to the treatment of sub-gridscale convection and cloud–radiation interactions. This sensitivity remains in idealized aquaplanet experiments with fixed surface temperatures. However, studies have not considered the role of cloud-radiative effects (CRE; atmospheric heating due to cloud–radiation interactions) in the sensitivity of the ITCZ to the treatment of convection. We use an atmospheric energy input (AEI) framework to explore how the CRE modulates the sensitivity of the ITCZ to convective mixing in aquaplanet simulations. Simulations show a sensitivity of the ITCZ to convective mixing, with stronger convective mixing favoring a single ITCZ. For simulations with a single ITCZ, the CRE maintains the positive equatorial AEI. To explore the role of the CRE further, we prescribe the CRE as either zero or a meridionally and diurnally varying climatology. Removing the CRE is associated with a reduced equatorial AEI and an increase in the range of convective mixing rates that produce a double ITCZ. Prescribing the CRE reduces the sensitivity of the ITCZ to convective mixing by 50%. In prescribed-CRE simulations, other AEI components, in particular the surface latent heat flux, modulate the sensitivity of the AEI to convective mixing. Analysis of the meridional moist static energy transport shows that a shallower Hadley circulation can produce an equatorward energy transport at low latitudes even with equatorial ascent.

## 1. Introduction

Tropical rainfall is often associated with a discontinuous zonal precipitation band commonly known as the intertropical convergence zone (ITCZ). The ITCZ migrates between the Northern and Southern Hemispheres with the seasonal cycle, with a zonal-mean, time-mean position of approximately 6°N (Schneider et al. 2014). The ITCZ is collocated with the ascending branch of the Hadley circulation, where strong moist convection leads to high rainfall. The upper branches of

the Hadley circulation typically transport energy poleward, away from the ITCZ. Recent studies have associated characteristics of the ITCZ with the energy transport by the Hadley circulation (Frierson and Hwang 2012; Donohoe et al. 2013; Adam et al. 2016; Bischoff and Schneider 2016).

A double ITCZ bias is prominent in current and previous generations of coupled general circulation models (GCMs; Li and Xie 2014; Oueslati and Bellon 2015). The ITCZ is too intense in the Southern Hemisphere (Lin 2007), resulting in two annual-mean, zonal-mean tropical precipitation maxima, one in each hemisphere. A bias

 Denotes content that is immediately available upon publication as open access.

*Corresponding author:* Joshua Talib, j.f.talib@pgr.reading.ac.uk



This article is licensed under a [Creative Commons Attribution 4.0 license](http://creativecommons.org/licenses/by/4.0/) (<http://creativecommons.org/licenses/by/4.0/>).

remains in atmosphere-only simulations with prescribed sea surface temperatures (SSTs) (Li and Xie 2014). Aquaplanet simulations provide an idealized modeling environment in which some complex boundary conditions in tropical circulation, such as land–sea contrasts and orography, are removed. However, aquaplanet configurations of GCMs coupled to a slab ocean produce a broad range of tropical precipitation mean states (Voigt et al. 2016); even prescribing zonally uniform SSTs does not resolve the intermodel variability (Blackburn et al. 2013).

#### *a. Modeling studies*

Characteristics of the simulated ITCZ are sensitive to the representation of cloud–radiation interactions (Fermepin and Bony 2014; Li et al. 2015; Harrop and Hartmann 2016). In the deep tropics the cloud radiative effect (CRE) warms the atmosphere (Allan 2011), with important effects on tropical circulation (Slingo and Slingo 1988; Crueger and Stevens 2015). The CRE is associated with a more prominent single ITCZ (Crueger and Stevens 2015; Harrop and Hartmann 2016; Popp and Silvers 2017). Both Harrop and Hartmann (2016) and Popp and Silvers (2017) investigated the association between the Hadley circulation and CRE in a range of aquaplanet simulations with and without the CRE. In all GCMs used, the CRE is associated with increased equatorial rainfall, an equatorward contraction of the ITCZ, and a strengthening of the mean meridional circulation. The authors emphasize different mechanisms by which the CRE promotes a single ITCZ. Harrop and Hartmann (2016) propose that the CRE warms the upper tropical troposphere, which reduces the convective available potential energy and restricts deep convection to the region of warmest SSTs, while Popp and Silvers (2017) argue that the CRE strengthens the Hadley circulation and moves the ITCZ equatorward, associated with increased moist static energy (MSE) advection by the lower branches of the Hadley circulation. The strengthening of the mean circulation is associated with the CRE meridional gradient, as the CRE is positive in the tropics and negative in the extratropics ( $\geq \pm 45^\circ$  latitude; Allan 2011). However, it should be noted that the CRE reduces total tropical-mean ( $\leq \pm 30^\circ$  latitude) precipitation due to reduced radiative cooling (Harrop and Hartmann 2016).

Across a hierarchy of models it has been shown that the simulation of tropical precipitation is sensitive to the representation of convection (Terray 1998; Frierson 2007; Wang et al. 2007; Chikira 2010; Mobis and Stevens 2012; Oueslati and Bellon 2013; Bush et al. 2015; Nolan et al. 2016). For example, variations in lateral entrainment and detrainment rates, which alter the representation of deep convection, affect the diurnal cycle of

precipitation over the Maritime Continent (Wang et al. 2007) and South Asian monsoon precipitation rates (Bush et al. 2015). Increasing convective mixing strengthens deep convection in convergence zones, associated with an increased moisture flux from subsidence regions (Terray 1998; Oueslati and Bellon 2013).

In full GCMs, complex surface characteristics and boundary conditions, including land–sea contrasts, orography, and SST gradients, make it challenging to understand the sensitivity of tropical precipitation to the representation of convection (Oueslati and Bellon 2013; Bush et al. 2015). Even in the absence of complex surface topography, aquaplanet studies have also shown that characteristics of tropical precipitation, in particular the location and intensity of the ITCZ, are sensitive to the sub-gridscale treatment of convection (Hess et al. 1993; Numaguti 1995; Chao and Chen 2004; Liu et al. 2010; Mobis and Stevens 2012). Mobis and Stevens (2012) studied the sensitivity of the ITCZ location to the choice of convective parameterization scheme in an aquaplanet configuration of the ECHAM GCM by comparing the Nordeng (1994) and Tiedtke (1989) schemes, which vary in their formulations of entrainment, detrainment and cloud base mass flux for deep convection. The Nordeng scheme, with a higher lateral entrainment rate, produced a single ITCZ, while the Tiedtke scheme produced a double ITCZ. The authors associate the location of maximum boundary layer MSE with the ITCZ location; they argue that mechanisms that control the boundary layer MSE are important to the sensitivity of the ITCZ to the representation of convection. The boundary layer MSE distribution is predominantly controlled by the surface winds, which are influenced by convective heating, allowing variations in convective heating to influence the ITCZ structure. The importance of the surface winds is further emphasized by simulations with prescribed surface winds in the computation of the surface fluxes (Mobis and Stevens 2012). These simulations lead to the conclusion that there is a strong association between surface turbulent fluxes and the ITCZ.

While the ITCZ has been shown to be sensitive to the CRE and the convective parameterization scheme, no study has separated these effects. This paper will analyze the sensitivity of the ITCZ to convective mixing in aquaplanet simulations using the Met Office Unified Model (MetUM), and the role of the CRE in this sensitivity.

#### *b. Atmospheric energy framework*

Literature based on a hierarchy of models, as well as reanalysis data and observations, concludes that the northward displacement of the ITCZ from the equator is anticorrelated with the northward cross-equatorial

atmospheric energy transport (Kang et al. 2008; Frierson and Hwang 2012; Donohoe et al. 2013). Bischoff and Schneider (2014) developed a diagnostic framework to relate the location of the ITCZ to this energy transport.

The zonal-mean atmospheric MSE budget is (Neelin and Held 1987)

$$[\text{AEI}] = \partial_t [\widehat{h}_e] + \partial_y [\widehat{vh}], \quad (1)$$

where AEI is the atmospheric energy input,  $vh$  is the meridional MSE flux ( $v$  is meridional wind;  $h$  is MSE),  $h_e$  is the moist enthalpy, square brackets denote zonal mean time mean, hat ( $\widehat{\cdot}$ ) represents a mass weighted vertical integral,  $\partial_y$  is the meridional derivative, and  $\partial_t$  is the time derivative. Local Cartesian coordinates are printed with  $y = a\phi$ , (where  $a$  is Earth's radius and  $\phi$  is latitude), but all calculations are performed in spherical coordinates. Bischoff and Schneider (2014) assume a statistically steady state ( $\partial_t [\widehat{h}_e] = 0$ ) and that  $[\widehat{vh}]$  in the tropics is dominated by the zonal-mean circulation and therefore  $[\widehat{vh}]$  equals zero at the ITCZ. Through performing a first-order Taylor expansion of the equatorial  $[\widehat{vh}]$ , Bischoff and Schneider (2014) derive the dependence of the ITCZ location on the equatorial MSE flux and equatorial AEI:

$$\delta \approx -\frac{1}{a} \frac{[\widehat{vh}]_0}{[\text{AEI}]_0}, \quad (2)$$

with the AEI defined as

$$[\text{AEI}] = [S] - [L] - [O], \quad (3)$$

where subscript 0 denotes the equatorial value,  $S$  is the net incoming shortwave radiation at the top of the atmosphere (TOA),  $L$  is the outgoing longwave radiation at the TOA, and  $O$  is the net downward flux at the surface. Bischoff and Schneider (2016) retain higher-order terms in the Taylor expansion to derive a framework for negative  $[\text{AEI}]_0$ . A negative  $[\text{AEI}]_0$  is associated with a double ITCZ as  $[\widehat{vh}]$  no longer increases with latitude; energy is transported equatorward at low latitudes to achieve equilibrium. A double ITCZ is associated with two off-equatorial energy flux equators, where the total meridional energy flux equals zero. Bischoff and Schneider (2016) derive an expression for the locations of a double ITCZ:

$$\delta \approx \pm \frac{1}{a} \left\{ -\frac{6([\text{AEI}]_0)}{\partial_{yy}([\text{AEI}]_0)} \right\}^{1/2} + \frac{[\widehat{vh}]_0}{2a([\text{AEI}]_0)}. \quad (4)$$

Note that Eq. (4) is from a corrigendum for the original paper.

Bischoff and Schneider (2014) explore the relationship derived in Eq. (2) using an idealized slab-ocean GCM with a prescribed oceanic heat transport. They investigate the effects of the  $[\text{AEI}]_0$  and the  $[\widehat{vh}]_0$  through varying the imposed equatorial ocean heat flux and the atmospheric longwave absorption. Changes in both  $[\text{AEI}]_0$  and  $[\widehat{vh}]_0$  affect the latitude of the ITCZ; this theoretical relationship is supported in observations and reanalyses (Adam et al. 2016). Bischoff and Schneider (2016) examine the double ITCZ framework [Eq. (4)] using a slab-ocean GCM and varying the tropical and extratropical components of the imposed ocean energy flux divergence. An increased tropical ocean energy flux divergence decreases the  $[\text{AEI}]_0$ . For double ITCZ scenarios and when  $[\widehat{vh}]_0$  is negligible, decreasing the  $[\text{AEI}]_0$  shifts the energy flux equator poleward. The diagnosed energy flux equators from Eqs. (2) and (4) are close to the simulated precipitation maxima, highlighting the association between the AEI and ITCZ.

However, Bischoff and Schneider (2014)'s definition of the  $[\text{AEI}]$  [Eq. (3)] is chosen as their simulations prescribe  $O$ , which allows only the TOA energy budget ( $S - L$ ) to vary. This constrains the AEI response to model perturbations, as surface radiation and turbulent fluxes are constrained at equilibrium, which could reduce the impact of surface-flux feedbacks on the ITCZ. We use atmosphere-only simulations with prescribed SSTs, allowing variations in the components of  $O$ . As our experiments do not have a closed surface energy balance and we are interested in cloudy-sky radiation AEI components, we choose to write the AEI as

$$[\text{AEI}] = [\text{SW}] + [\text{LW}] + [H], \quad (5)$$

where SW and LW represent the net atmospheric heating from shortwave and longwave radiation, respectively, and  $H$  denotes the atmospheric heating from surface sensible and latent heat fluxes. Both fixed SST and prescribed  $O$  frameworks misrepresent the real climate system by restricting air-sea coupled feedbacks (discussed further in section 4). From an AEI perspective, Mobis and Stevens (2012) severely constrain  $H$  in a subset of experiments by prescribing the surface winds when computing the surface fluxes. This reduces the sensitivity of the ITCZ to the convective parameterization scheme.

Previous research on the response of the simulated ITCZ to variations in the sub-gridscale representation of convection has not considered the role of the CRE or used an energy budget framework like that proposed by Bischoff and Schneider (2014). We hypothesize that the sensitivity of the ITCZ to these factors can be linked to variations in AEI and  $[\widehat{vh}]$ .

TABLE 1. Simulations varying  $f_{dp}$  with cloud-radiation interactions on (CRE-on) and off (CRE-off). F1.13 is the default integration for GA6.0.

$f_{dp}$	CRE-on	CRE-off
0.28	F0.28	F0.28NC
0.57	F0.57	F0.57NC
0.85	F0.85	F0.85NC
1.13	F1.13	F1.13NC
1.70	F1.70	F1.70NC

## 2. Methodology

We use variations of an N96 (1.25° latitude  $\times$  1.875° longitude) aquaplanet configuration of the Met Office Unified Model Global Atmosphere 6.0 (GA6.0) configuration (Walters et al. 2017). The deep convective parameterization scheme is an altered form of the mass flux scheme in Gregory and Rowntree (1990), including a convective available potential energy closure based on Fritsch and Chappell (1980) and a mixing detrainment rate dependent on the relative humidity (Derbyshire et al. 2004). Unless noted, all simulations are run for three years with a “Qobs” SST profile (Neale and Hoskins 2001), with the first 60 days discarded as spinup.

### Simulations performed

To explore the sensitivity of the simulated ITCZ to convective mixing, we perform five simulations varying the lateral entrainment ( $\varepsilon$ ) and detrainment ( $d_m$ ) rates for deep-level convection (Table 1). In GA6.0 these rates are

$$\varepsilon = 4.5f_{dp} \frac{p(z)\rho(z)g}{p_*^2} \quad \text{and} \quad (6)$$

$$d_m = 3.0(1 - \text{RH})\varepsilon. \quad (7)$$

Both  $\varepsilon$  and  $d_m$  are given as a fractional mixing rate per unit length ( $\text{m}^{-1}$ ). In Eqs. (6) and (7),  $p$  and  $p_*$  are pressure and surface pressure (Pa),  $\rho$  is density ( $\text{kg m}^{-3}$ ),  $g$  is gravitational acceleration ( $\text{m s}^{-2}$ ),  $f_{dp}$  is a constant with the default value of 1.13, and RH is relative humidity. We control  $\varepsilon$  and  $d_m$  by scaling  $f_{dp}$  to five values between 0.25 and 1.5 times the default value: 0.28 (F0.28), 0.57 (F0.57), 0.85 (F0.85), 1.13 (F1.13), or 1.70 (F1.70).

To explore the influence of the CRE on the sensitivity of the ITCZ to convective mixing we perform a companion set of experiments with cloud-radiation interactions removed: F0.28NC, F0.57NC, F0.85NC, F1.13NC, and F1.70NC (Table 1). Cloud-radiation interactions are removed by setting cloud liquid and cloud ice to zero in the radiation scheme.

Finally, a third set of simulations use a prescribed CRE (Table 2) to investigate the relative importance of

TABLE 2. Simulations with a prescribed climatology of the CRE diurnal cycle. PC1.13 and PC0.57 represent the prescribed CRE diurnal cycle from a 1-year simulation where  $f_{dp}$  equals 1.13 or 0.57, respectively.

$f_{dp}$	PC1.13	PC0.57
1.13	F1.13PC1.13	F1.13PC0.57
0.57	F0.57PC1.13	F0.57PC0.57

$f_{dp}$  and the CRE to characteristics of the ITCZ. The four simulations have a prescribed, diurnally varying CRE vertical profile computed from a single-year simulation with  $f_{dp}$  equal to 0.57 or 1.13 (PC0.57 and PC1.13, respectively). The CRE is prescribed using cloudy-sky upward and downward fluxes at each model level at every model time step. The diurnally varying CRE profile is computed as a hemispherically symmetric and zonally uniform composite of the climatological diurnal cycle at each grid point, referenced to local solar time. Two of the four simulations prescribe a CRE at a different  $f_{dp}$  constant from that in the simulation (F1.13PC0.57, F0.57PC1.13), while the other two simulations use a CRE from the same  $f_{dp}$  value to assess the sensitivity to prescribed cloud-radiation interactions (F1.13PC1.13, F0.57PC0.57).

## 3. Results

### a. Sensitivity of the ITCZ to the convective mixing

Figure 1a shows the sensitivity of the ITCZ to  $f_{dp}$  with a single ITCZ at higher values (F1.13, F1.70). Reducing  $f_{dp}$  promotes a double ITCZ, with peak precipitation farther away from the equator (F0.28, F0.57). F0.85 has a marginal double ITCZ with no substantial difference between equatorial and off-equatorial precipitation. Decreasing  $f_{dp}$  is associated with a weaker horizontal gradient of the mass meridional streamfunction (Fig. 2). F0.28 is the only simulation to show a reversed Hadley circulation in the deep tropics (Fig. 2e), associated with upper-level zonal-mean equatorial subsidence, typical of a double ITCZ. F0.57 meanwhile has a typical double ITCZ structure in precipitation but not in the mass meridional streamfunction (Figs. 1a and 2d), which we refer to as a “split ITCZ”: two off-equatorial precipitation maxima and two ascending branches of the Hadley circulation, without any substantial zonal-mean subsidence equatorward of the precipitation maxima.

Convective mixing reduces the difference in MSE between a convective plume, determined by the boundary layer MSE, and the free troposphere (Mobis and Stevens 2012), which reduces the buoyancy of the convective



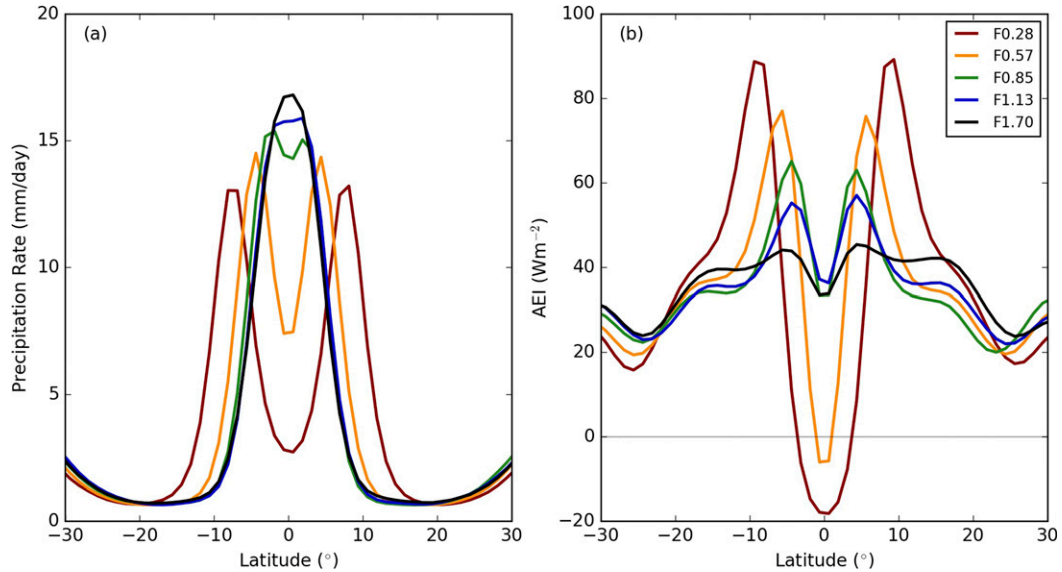


FIG. 1. Zonal-mean, time-mean (a) precipitation rates ( $\text{mm day}^{-1}$ ) and (b) AEI ( $\text{W m}^{-2}$ ) in simulations where  $f_{dp}$  is varied.

plume. Assuming the sensitivity of the environmental saturated MSE to  $f_{dp}$  is small, the depth of convection will depend on the boundary layer MSE and  $f_{dp}$ . Decreasing  $f_{dp}$  will deepen convection for a constant boundary layer MSE, and reduce the minimum boundary layer MSE at which deep convection occurs. Following weak-temperature gradient arguments (e.g., Sobel et al. 2001) and assuming a small meridional gradient in free-tropospheric tropical temperature, and hence a small gradient in the saturated MSE across the deep tropics, the reduced minimum boundary layer MSE needed for deep convection strengthens convection in off-equatorial tropical latitudes over cooler SSTs. Stronger off-equatorial deep convection decreases equatorward low-level winds in the deep tropics, reducing equatorial boundary layer MSE. Hence, decreasing  $f_{dp}$  is associated with a poleward ITCZ shift and promotes a double ITCZ. Similar arguments can be made for higher  $f_{dp}$  promoting a single ITCZ.

The sensitivity of the ITCZ to  $f_{dp}$  is associated with AEI changes (Fig. 1b), with a change from a single (F1.13) to a double/split ITCZ (F0.28/F0.57) associated with a decrease in the  $[\text{AEI}]_0$  (Figs. 3d,e). Simulations with a single (double) ITCZ in precipitation have a positive (negative)  $[\text{AEI}]_0$  (Fig. 1b), in agreement with Bischoff and Schneider (2014). Changes in cloudy-sky radiation and latent heat flux are the dominant components of AEI changes (blue and orange lines, respectively, in Fig. 3). In F1.13 the total CRE peaks at approximately  $60 \text{ W m}^{-2}$  at the equator and reduces to zero around  $15^\circ$  latitude (blue line in Fig. 3b). This equatorial warming comes almost entirely from the

longwave CRE, which dominates the total CRE equatorward of  $10^\circ$  latitude (not shown). In the subtropics,  $20^\circ$  to  $30^\circ$  latitude, low clouds contribute to a negative CRE of  $\approx 2 \text{ W m}^{-2}$ , as longwave cooling from boundary layer clouds is greater than the shortwave heating. Without the CRE contribution to the  $[\text{AEI}]_0$  in F1.13,  $[\text{AEI}]_0$  would be negative, suggesting that the CRE maintains the single ITCZ. Removing the CRE from the AEI in F1.13 would give an  $[\text{AEI}]_0$  of  $-25.7 \text{ W m}^{-2}$ , assuming that no other AEI components change. Using Bischoff and Schneider (2016)'s framework, Eq. (4), with values for AEI once removing the CRE and assuming that  $[\widehat{v\bar{h}}]_0 \simeq 0 \text{ W m}^{-1}$  (associated with a hemispherically symmetric atmospheric circulation), predicts a double ITCZ at  $\pm 5.6^\circ$  latitude.

The split ITCZ in F0.57 is associated with a substantially reduced equatorial CRE and an increased off-equatorial CRE (Fig. 3d). We chose CRE profiles from one year of F0.57 and F1.13 for our prescribed-CRE simulations (Table 2), as these two simulations show CRE profiles typical of a double and single ITCZ, respectively; these simulations are analyzed in section 3d. As the Hadley circulation and ITCZ are associated with the AEI, and the CRE plays a substantial role in AEI changes when varying  $f_{dp}$ , we hypothesize that prescribing the CRE will reduce or remove the sensitivity of the AEI and ITCZ to  $f_{dp}$ .

#### b. Sensitivity of the ITCZ to convective mixing with no cloud radiative effect

To test our hypothesis above, we first analyze simulations with the CRE removed (Table 1), similar to

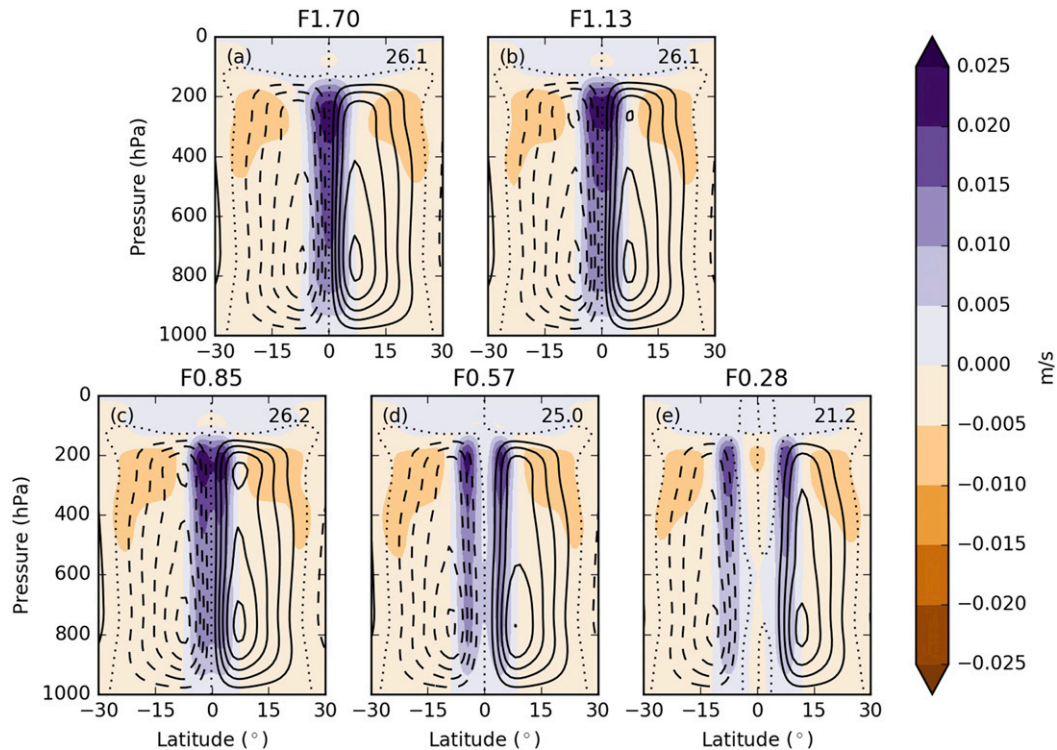


FIG. 2. Zonal-mean, time-mean mass meridional streamfunction ( $\text{kg s}^{-1}$ ) (lined contours) and vertical wind speed ( $\text{m s}^{-1}$ ) (filled contours) for (a) F1.70, (b) F1.13, (c) F0.85, (d) F0.57, and (e) F0.28. Lined contours are in intervals of  $5 \times 10^{10}$ , with dashed contours representing negative values. Dotted contour is zero value. Maximum value of the mass meridional streamfunction printed in top right-hand corner of each subplot.

Harrop and Hartmann (2016). Figures 4a and 5 show the zonal-mean precipitation and mass meridional streamfunction respectively in simulations with no CRE (Table 1). Removing the CRE at  $f_{\text{dp}} = 1.13$  (F1.13NC) leads to a switch from a single to a split ITCZ, and  $\approx 20\%$  weakening of the Hadley circulation (Figs. 4a and 5b).

Similar to Harrop and Hartmann (2016), removing the CRE cools the tropical ( $\leq 30^\circ$  latitude) upper troposphere, destabilizing the atmosphere and reducing the environmental saturated MSE. For a fixed boundary layer MSE and convective mixing rate, removing the CRE deepens convection as the buoyancy of a convective plume increases relative to the saturated MSE of the environment. Hence, removing the CRE reduces the minimum boundary layer MSE for deep convection, strengthening off-equatorial convection over cooler SSTs. Stronger off-equatorial convection decreases equatorward low-level winds in the deep tropics, reducing equatorial boundary layer MSE and promoting a double ITCZ. This mechanism is similar to that proposed for the sensitivity of the ITCZ to  $f_{\text{dp}}$  (section 3a). However, when removing the CRE changes in the environmental saturated MSE play the dominant role, while for the sensitivity of the

ITCZ to  $f_{\text{dp}}$ , changes in the convective parcel MSE dominate.

The weaker Hadley circulation and double ITCZ in precipitation in F1.13NC is consistent with AEI changes. In F1.13NC removing CRE reduces the  $[\text{AEI}]_0$  by  $\approx 45 \text{ W m}^{-2}$ , leading to a negative  $[\text{AEI}]_0$ , and increases the subtropical AEI by up to  $15 \text{ W m}^{-2}$  ( $20^\circ$  to  $45^\circ$  latitude) (Fig. 6f). Across the deep tropics the AEI change is not equal to the CRE diagnosed from F1.13, due to increased turbulent and clear-sky fluxes. These increased fluxes, associated with an equatorward shift of the ITCZ, partially offset the reduction in  $[\text{AEI}]_0$ . Hence, the predicted location of the double ITCZ in section 3a when removing the CRE overestimated the poleward shift of the ITCZ. Removing the CRE reduces tropical-domain ( $\leq \pm 30^\circ$  latitude) AEI, which is associated with increased AEI at higher latitudes to maintain equilibrium. Our simulations are consistent with the suggested mechanisms proposed by Popp and Silvers (2017): the ITCZ is located at the maximum boundary layer MSE, and a weaker meridional circulation is associated with a reduced AEI gradient.

At all  $f_{\text{dp}}$  removing the CRE reduces the maximum precipitation rate, weakens the Hadley circulation



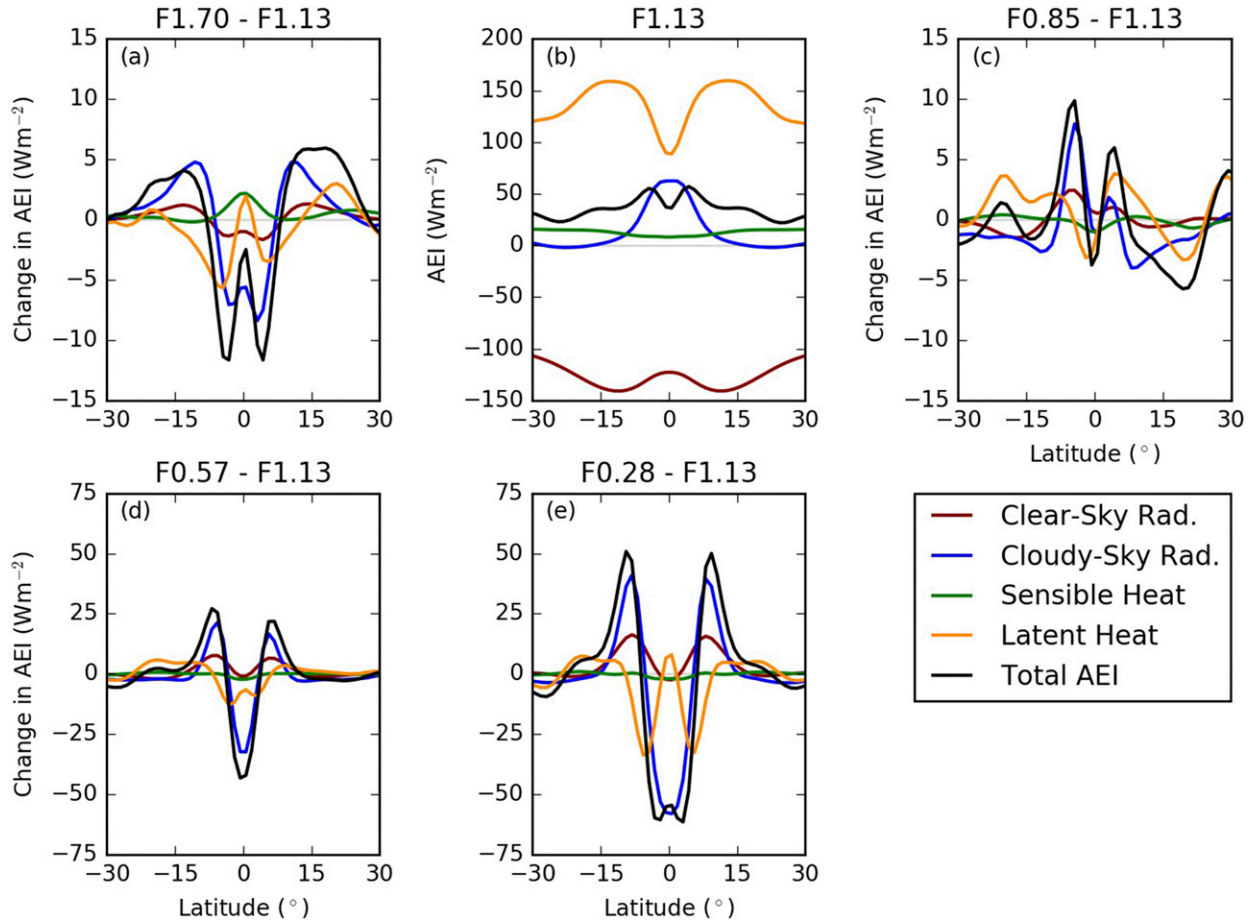


FIG. 3. Zonal-mean, time-mean AEI components ( $\text{W m}^{-2}$ ), showing (b) F1.13 and, in all other panels, the change in AEI components compared to F1.13 for (a) F1.70; (c) F0.85, (d) F0.57, and (e) F0.28. The red line is the clear-sky component; the blue line is the cloudy-sky component. Green and orange lines represent the sensible and latent heat flux, respectively, and the black line is the total change in AEI. Note that (a) and (c) have axis limits of  $-15$  and  $15 \text{ W m}^{-2}$ , while (d) and (e) have limits of  $-75$  and  $75 \text{ W m}^{-2}$ .

(cf. Figs. 1a and 4a), and moves the latitude of peak precipitation poleward (Fig. 7a). The sensitivity of the ITCZ structure to removing the CRE depends on the convective mixing rate: either a broader single ITCZ (F1.70NC), a poleward shift of a double/split ITCZ (F0.28NC and F0.57NC) or a switch from a single to a split/double ITCZ (F0.85NC and F1.13NC). Removing the CRE cools the upper troposphere and reduces the boundary layer MSE required for deep convection. This increases the  $f_{\text{dp}}$  value at which the ITCZ transitions from single to split/double.

Removing the CRE changes, but does not remove, the sensitivity of the ITCZ to  $f_{\text{dp}}$ . Quantifying the apparent effect of the CRE on the sensitivity of the ITCZ to  $f_{\text{dp}}$  is difficult, as the effect depends on both the range of  $f_{\text{dp}}$  considered and the metric used (Fig. 7). When an off-equatorial ITCZ is simulated in CRE-off simulations ( $0.28 \leq f_{\text{dp}} \leq 1.13$ ), including the CRE increases the

sensitivity of the ITCZ location to  $f_{\text{dp}}$  by  $\approx 30\%$  (comparing the slopes of the solid regression lines in Fig. 7a). However, because F1.70NC has a single ITCZ, including the CRE cannot shift the ITCZ equatorward. Hence, when  $0.28 \leq f_{\text{dp}} \leq 1.70$  the change in sensitivity reduces to nearly zero (comparing the slopes of the dashed lines). The reduction in sensitivity also depends on the chosen metric; for instance, the maximum precipitation rate has a negligible sensitivity to  $f_{\text{dp}}$  in CRE-off simulations but a substantial sensitivity in CRE-on simulations (Fig. 7b), highlighting that the CRE has a positive feedback on convection as increasing  $f_{\text{dp}}$  is associated with an increased CRE (Fig. 8).

Increasing  $f_{\text{dp}}$  is associated with an increased tropical-domain CRE (Fig. 8), which is counterintuitive as one might expect that increasing  $f_{\text{dp}}$  will lead to lower cloud tops and hence a reduced CRE. However, the maximum cloud top height at the ITCZ is insensitive to  $f_{\text{dp}}$  (not

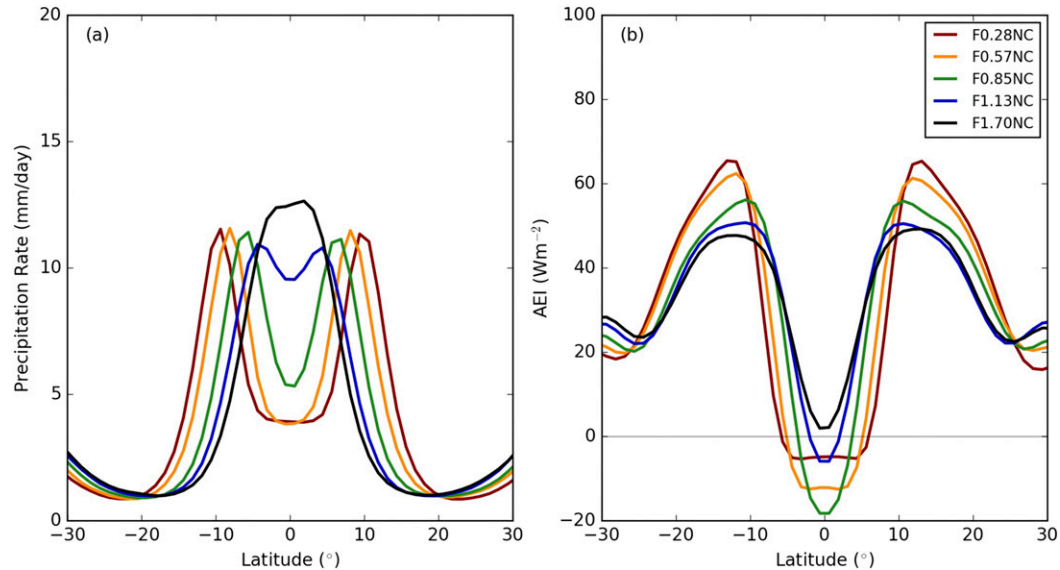


FIG. 4. Zonal-mean, time-mean (a) precipitation rates ( $mm day^{-1}$ ) and (b) AEI ( $W m^{-2}$ ) in CRE-off simulations where  $f_{dp}$  is varied.

shown), but the minimum temperature where the cloud fraction goes to zero (cloud top temperature) is sensitive to  $f_{dp}$  in both CRE-on and CRE-off simulations (Fig. 8). The cloud-top temperature decreases as  $f_{dp}$  increases

(Fig. 8), associated with a cooler upper-troposphere. Furthermore, the increase in SST at the ITCZ location, associated with equatorward contraction of the ITCZ, also contributes to an increased CRE at higher  $f_{dp}$ .

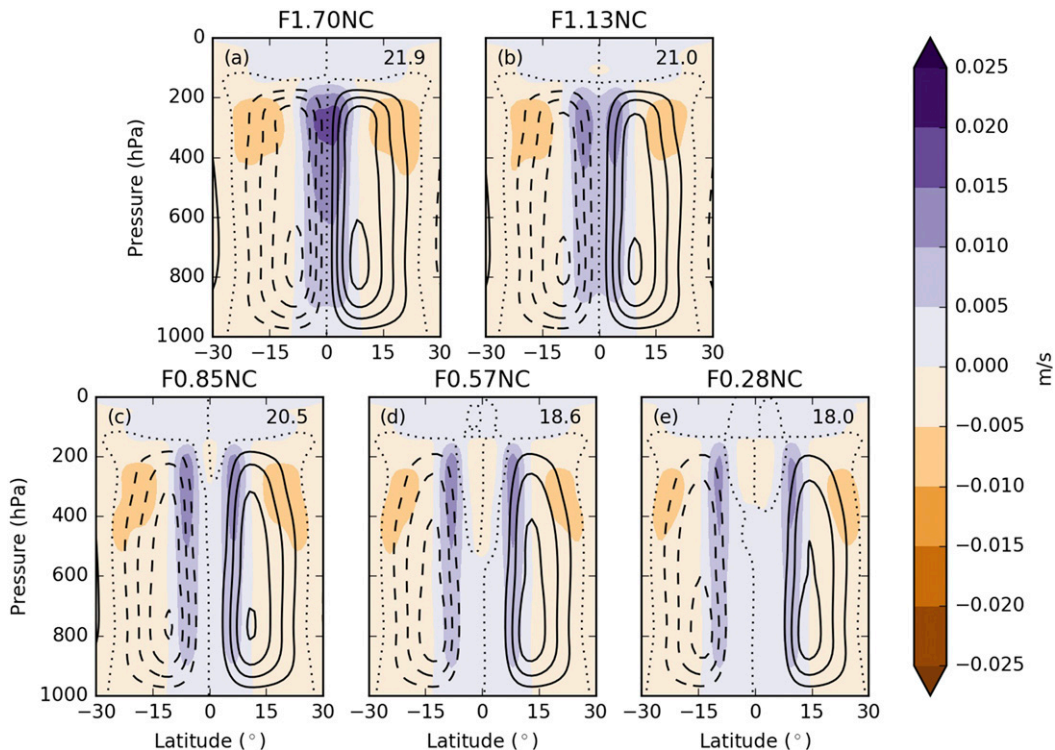


FIG. 5. Zonal-mean, time-mean mass meridional streamfunction ( $kg s^{-1}$ ) (lined contours) and vertical wind speed ( $m s^{-1}$ ) (filled contours), for (a) F1.70NC, (b) F1.13NC, (c) F0.85NC, (d) F0.57NC, and (e) F0.28NC. Lined contours are in intervals of  $5 \times 10^{10}$ , with dashed contours representing negative values. Dotted contour is zero value. Maximum value of the mass meridional streamfunction printed in top right-hand corner of each subplot.

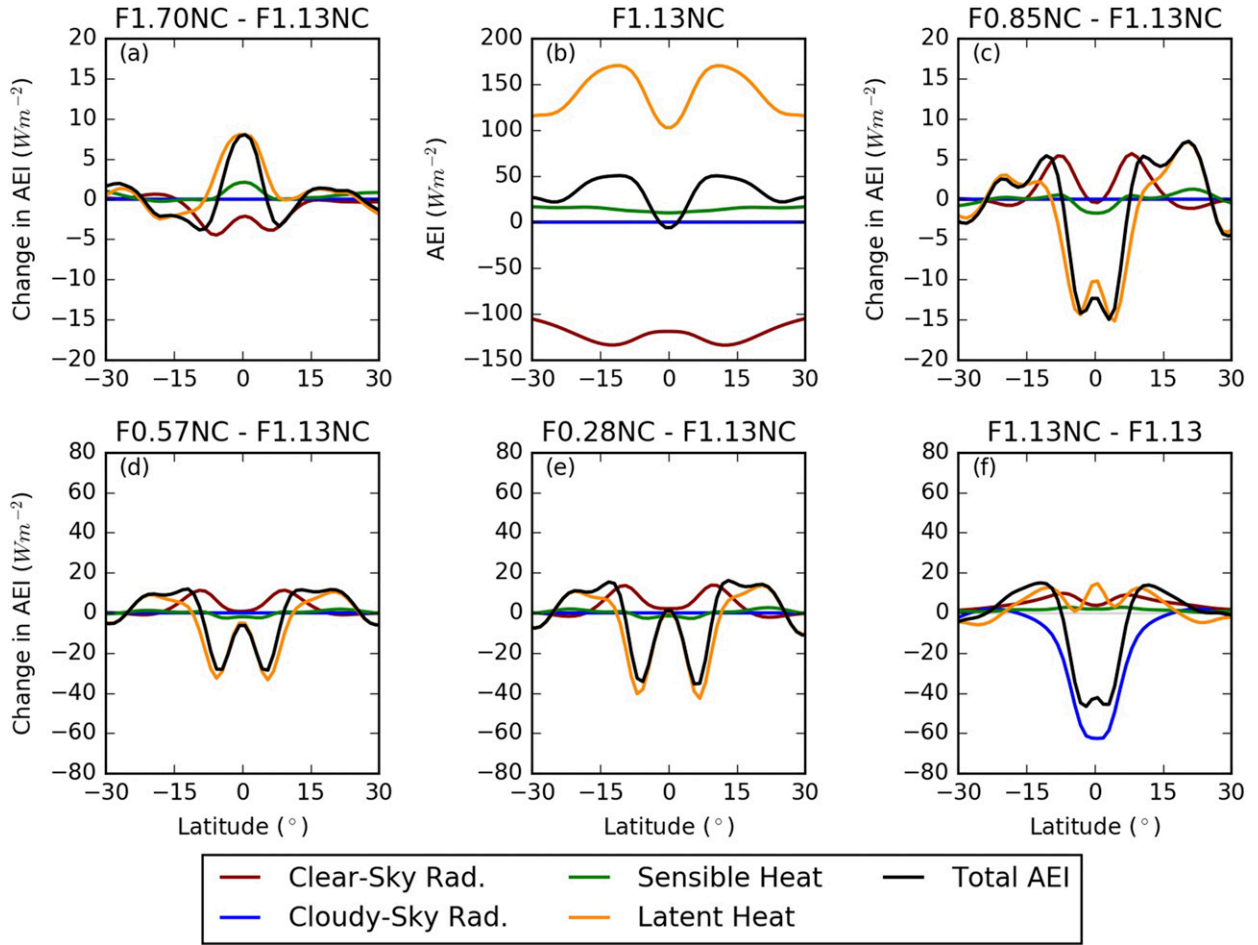


FIG. 6. Zonal-mean, time-mean AEI components ( $\text{W m}^{-2}$ ), showing (b) F1.13NC, and, in all other panels, the change in AEI components compared to F1.13NC for (a) F1.70NC, (c) F0.85NC, (d) F0.57NC, and (e) F0.28NC. (f) Change in AEI components when removing cloud-radiation interactions at  $f_{dp} = 1.13$  (F1.13NC-F1.13). Note, (a) and (c) have axis limits of  $-20$  and  $20 \text{ W m}^{-2}$  while (d)–(f) have limits of  $-80$  and  $80 \text{ W m}^{-2}$ .

Removing the CRE decreases the sensitivity of the AEI to  $f_{dp}$  (comparing Figs. 1b and 4b). The reduced sensitivity of the AEI is associated with a reduced sensitivity of the ITCZ. Latent heat flux variations account for most of the remaining AEI sensitivity to  $f_{dp}$  (Fig. 6). In simulations with a double ITCZ (F0.28NC, F0.57NC, and F0.85NC), changes in the latent heat flux and AEI have a bimodal structure, indicating reduced latent heat flux at the location of maximum precipitation in F1.13NC (Figs. 6c–e). Changes in the latent heat flux are predominantly controlled by alterations in near-surface wind speed rather than changes in near-surface specific humidity (not shown).

Simulations so far agree with the association in Bischoff and Schneider (2016) between a negative  $[\text{AEI}]_0$  and a double ITCZ. However, the negative  $[\text{AEI}]_0$  in F0.57, F0.85NC, and F1.13NC requires an equatorward transport of energy at low latitudes, but the mean mass meridional streamfunction suggests a poleward transport of energy

(Figs. 2b and 5c,d). In the following subsection we discuss mechanisms for an equatorward energy transport.

### c. Mechanisms responsible for an equatorward energy transport

To better understand the response of the mean circulation, associated with ITCZ changes, to varying  $f_{dp}$  and removing the CRE, we partition the divergence of the MSE flux  $\partial_y[\widehat{v\overline{h}}]$  into two components: the mean circulation  $\partial_y([\widehat{v}][\widehat{h}])$  and the eddy contribution  $\partial_y[\widehat{v\overline{h}}] - \partial_y([\widehat{v}][\widehat{h}])$ . In these simulations it has not been possible to close the atmospheric energy budget (1) due to local energy conservation issues (discussed further in section 4); however, the sign of the  $[\text{AEI}]_0$  is consistent with the sign of the  $\partial_y[\widehat{v\overline{h}}]$  in simulations so far. In all simulations the eddy contribution to the meridional MSE flux is substantial across the tropics, highlighting that the mean atmospheric circulation is not solely responsible for transporting energy. Furthermore, one should not necessarily assume a correspondence

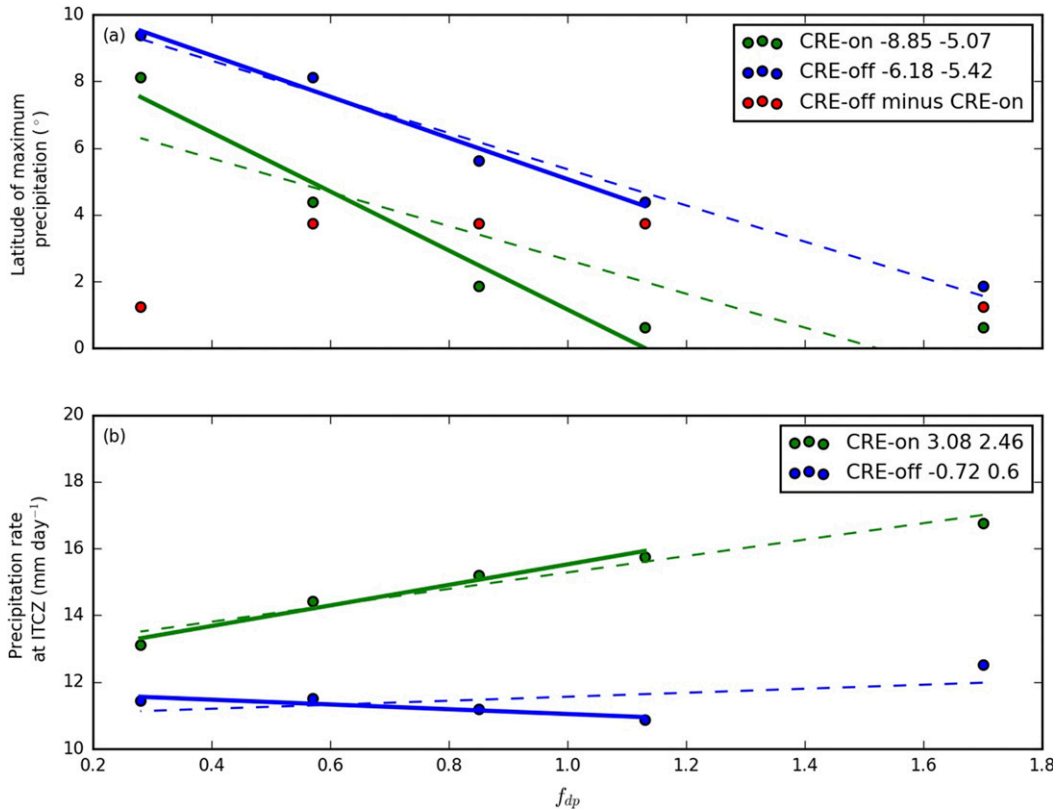


FIG. 7. Diagnostics for determining the sensitivity of the ITCZ to  $f_{dp}$  in CRE-on (green) and CRE-off (blue) simulations. (a) Latitude of maximum precipitation ( $^{\circ}$ ). (b) Precipitation rate at ITCZ ( $\text{mm day}^{-1}$ ). Four regression lines are plotted in each subplot. Solid lines where  $0.28 \leq f_{dp} \leq 1.13$  and dashed lines where  $f_{dp} \leq 1.70$ . The slope of each regression line is printed in the legend. The first value indicates where  $0.28 \leq f_{dp} \leq 1.13$  and the second value where  $f_{dp} \leq 1.70$ .

between the required MSE transport and the transport by the mean meridional circulation. In simulations with a single (double) ITCZ, both the mean circulation and eddies transport energy poleward (equatorward) at low latitudes. In F0.57, which has a negative  $[AEI]_0$  and a split ITCZ, equatorward transport of energy at low latitudes is achieved solely by eddies. When  $f_{dp} = 0.85$  and 1.13, a change in the sign of the energy transport by the mean circulation  $\partial_y([\hat{v}][\hat{h}])$  occurs at low latitudes when removing the CRE; however, there is still equatorial ascent across most of the troposphere (Figs. 5b,c). To understand the sensitivity of the mean circulation to removing the CRE at these convective mixing rates, we partition the change in the MSE flux  $[\hat{v}][\hat{h}]$  into mean circulation changes and MSE variations.

First, the meridional mass flux, denoted by  $V$ , in F1.13NC ( $V_e$ ) is partitioned into two components:

$$V_e = V_c(1 + \alpha) + V_r$$

$$\text{where } \alpha = \frac{V_e V_c}{V_c V_c} - 1. \quad (8)$$

Subscripts  $c$  and  $e$  represent the zonal-mean, time-mean value of the control and experiment simulation (in this case F1.13 and F1.13NC respectively). Also,  $\alpha$  is a globally uniform scaling term calculated using the dot product of the meridional mass fluxes in the tropics ( $30^{\circ}\text{N}$  to  $30^{\circ}\text{S}$ ). We account for variations in density in  $V$ . The term  $V_c(1 + \alpha)$  represents a change in strength of the control circulation;  $V_r$  represents a change in circulation structure. Next, the MSE ( $c_p T + gz + Lq$ ) in the experiment simulation  $h_e$  is written as

$$h_e = h_c + h_p, \quad (9)$$

where subscript  $p$  represents the zonal-mean, time-mean difference between the two simulations. The change in the MSE flux between the experiment and control simulation can therefore be written as

$$V_e h_e - V_c h_c = \alpha V_c h_c + V_r h_c + V_c h_p + (\alpha V_c + V_r) h_p. \quad (10)$$

Each term in Eq. (10) represents a mechanism by which  $vh$  can vary:  $\alpha V_c h_c$  represents circulation intensity changes,  $V_r h_c$  represents changes in circulation structure,  $V_c h_p$  represents MSE profile changes, and  $(\alpha V_c + V_r) h_p$ ,



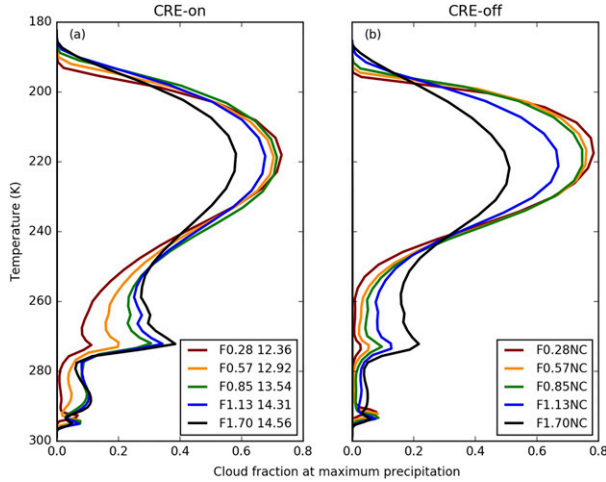


FIG. 8. Zonal-mean, time-mean cloud fraction against temperature (K) at latitude of maximum precipitation, for (a) CRE-on and (b) CRE-off simulations. Printed in the legend is the tropical-domain average CRE ( $\text{W m}^{-2}$ ) for CRE-on simulations.

represents MSE profile changes correlated with changes in circulation structure and strength.

Three out of the four mechanisms are important in reducing the poleward MSE transport by the

Hadley circulation in F0.85NC and F1.13NC (Fig. 9): a reduction in Hadley circulation strength (Fig. 9e), a shallower mean circulation (Fig. 9f), and a reduced MSE export at the top of the Hadley circulation due to lower MSE associated with upper-tropospheric cooling (Fig. 9g). MSE profile changes correlated with changes in circulation strength and intensity  $[(\alpha V_c + V_r)h_p]$  are small compared to the other three mechanisms (Fig. 9h). As changes in circulation strength  $(\alpha V_c h_c)$  cannot change the direction of energy transport, the reduced upper-tropospheric MSE ( $V_c h_p$ ) and shallower Hadley circulation ( $V_r h_c$ ) must be responsible for the change in energy transport direction by the mean circulation. At the equator, circulation strength changes  $(\alpha V_c h_c)$  contribute  $\approx 16\%$  of the reduced  $\partial_y([\hat{v}][\hat{h}])$ ; reduced MSE export by the upper branch of the mean circulation ( $V_c h_p$ ) and a shallower Hadley circulation ( $V_r h_c$ ) contribute approximately 34% and 50%, respectively (not shown). Therefore, at certain convective mixing rates, in our case when  $f_{\text{dp}} = 0.85$  and 1.13, removing the CRE is not associated with a substantial double ITCZ in the mass meridional streamfunction, even though MSE is transported equatorward at low latitudes and the  $[AEI]_0$  is negative. Similar behavior has also been concluded by Popp and

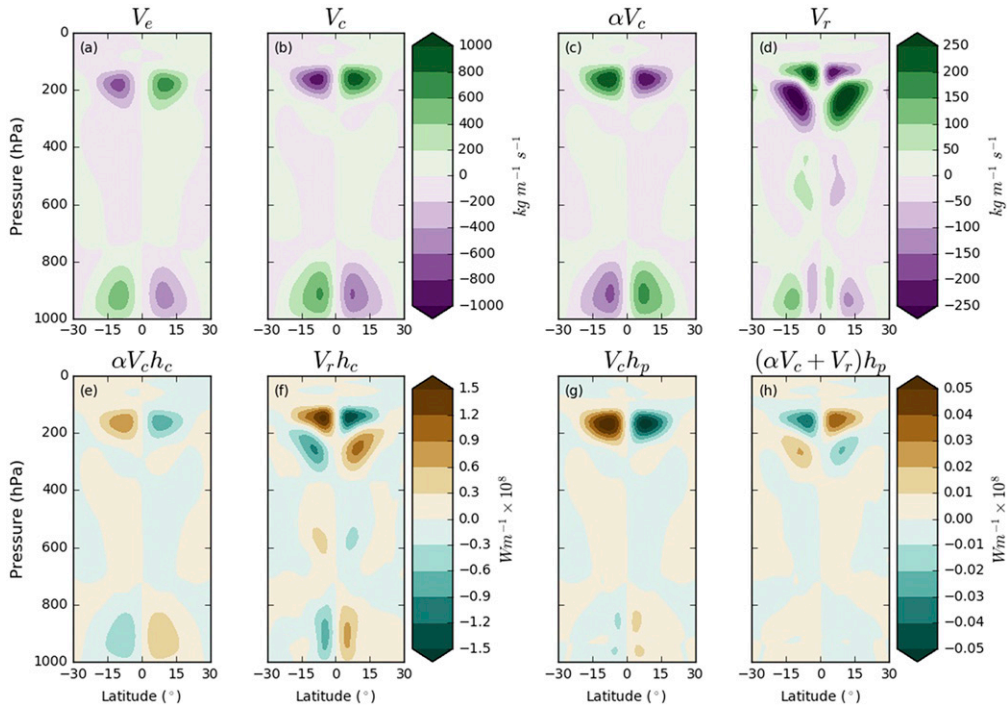


FIG. 9. (a),(b) Meridional mass flux ( $\text{kg m}^{-1} \text{s}^{-1}$ ) in F1.13NC and F1.13 respectively. (c),(d) Change in meridional mass flux due to change in circulation strength and change in meridional wind, respectively. Also shown are components of MSE flux change ( $\text{W m}^{-1}$ ), Eq. (10), due to (e) circulation intensity changes  $\alpha V_c h_c$ , (f) changes in circulation structure  $V_r h_c$ , (g) MSE profile changes  $V_c h_p$ , and (h) MSE changes correlated with changes in circulation structure and strength  $(\alpha V_c + V_r)h_p$ . Analysis is explained in section 3c.



Silvers (2017), who found that in certain simulations the zero mass meridional streamfunction remained at the equator even when the  $[AEI]_0$  was negative.

Removing the CRE and varying  $f_{dp}$  are associated with substantial AEI changes that require MSE transport variations. In the two sets of simulations discussed so far, we identified three mechanisms to transport MSE equatorward at low latitudes; which mechanisms dominate depends on the CRE and  $f_{dp}$ . First, in F0.28, F0.28NC, and F0.57NC, subsidence across the equatorial region is associated with an equatorward MSE flux at low latitudes (Figs. 2e and 5d,e). Second, eddy energy transport plays a role in the equatorward MSE flux in F0.28, F0.57, F0.28NC, F0.57NC, and F0.85NC. Third, in F0.85NC and F1.13NC a shallower Hadley circulation and reduced upper-tropospheric MSE reduce the MSE exported in the upper branches of the mean circulation, resulting in a net equatorward MSE transport. All other simulations (F0.85, F1.13, F1.70, and F1.70NC) have a single ITCZ associated with a positive  $[AEI]_0$  and poleward MSE transport at low latitudes.

#### d. Sensitivity of the ITCZ to convective mixing with a prescribed cloud radiative effect

To further understand the role of the CRE on the sensitivity of the ITCZ to convective mixing, we perform prescribed-CRE simulations and vary  $f_{dp}$  (Table 2). The prescribed CRE is diagnosed from single-year simulations with  $f_{dp}$  equal to 1.13 or 0.57 (section 2). The effect of prescribing the diurnal cycle of the CRE in a simulation with the same  $f_{dp}$  is minimal; for example, the ITCZ is similar in F1.13PC1.13 and F1.13 (Figs. 1 and 10). Hence, we only discuss the mean circulation in F1.13PC0.57 and F0.57PC1.13 (Figs. 11a,c).

Similar to CRE-off simulations, the sensitivity of the ITCZ to  $f_{dp}$  reduces in prescribed CRE simulations (Fig. 10a) compared to CRE-on simulations (Fig. 1a), associated with a reduced sensitivity of the AEI to  $f_{dp}$  (Figs. 10b and 12a,c). The prescribed CRE heating acts as a fixed MSE source, which requires an increase in MSE export and hence increased convective activity. In PC1.13 simulations the CRE maximizes at the equator, which is associated with increased equatorial convective activity and a single ITCZ. In PC0.57 simulations on the other hand, the CRE peaks off the equator and promotes a double ITCZ. The root-mean-square difference of tropical precipitation and the mass meridional streamfunction illustrates that prescribing the CRE reduces the sensitivity of the ITCZ and Hadley circulation to  $f_{dp}$  by  $\approx 50\%$  (Table 3). While the CRE plays a role in the sensitivity of the ITCZ to convective

mixing (e.g., comparing F1.13PC1.13 and F1.13PC0.57 in Fig. 10a), the ITCZ and Hadley circulation are still sensitive to  $f_{dp}$ . For example, reducing  $f_{dp}$  (F0.57PC1.13) leads to a weakening in the upper branch of the mean circulation while changing the prescribed CRE (F1.13PC0.57) intensifies the upper branch of the Hadley circulation as the higher  $f_{dp}$  value is associated with a cooler upper-troposphere, and hence an intensified upper branch of the mean circulation is required for similar MSE transport (comparing F1.13 in Fig. 2b to F0.57PC1.13 and F1.13PC0.57 in Figs. 11c and 11a, respectively). The response of convection to changes in convective mixing is partially offset by the effect of prescribing the location of the CRE.

As in CRE-off simulations, AEI changes in prescribed-CRE simulations when varying  $f_{dp}$  are predominantly driven by latent heat flux variations. For example, between F1.13PC1.13 and F0.57PC1.13, the equatorial latent heat flux reduces while the off-equatorial latent heat flux increases (Fig. 12a). These changes are partially offset by changes in the clear-sky radiation, associated with a decrease in the TOA outgoing longwave radiation, due to an increase in atmospheric water vapor content. As changes in the ITCZ are associated with AEI changes, we conclude that the remaining sensitivity of the ITCZ to  $f_{dp}$  in prescribed CRE simulations is associated with latent heat flux variations. In simulations where the prescribed CRE is varied but the same  $f_{dp}$  value is used, AEI changes are mostly associated with cloudy-sky radiation (Fig. 12b,d). However, latent heat flux variations are of the same order of magnitude as when varying  $f_{dp}$ . Using the same technique described in section 3c, we conclude that a shallower, weaker Hadley circulation is primarily responsible for changes in the MSE transport by the mean circulation when reducing  $f_{dp}$  or changing the prescribed CRE from PC1.13 to PC0.57 (not shown).

F1.13PC0.57 and F0.57PC1.13 have similar split ITCZs (Fig. 10a), yet very different AEI profiles (Figs. 10b and 11b,d). F0.57PC1.13 highlights that a double ITCZ in precipitation does not require a negative  $[AEI]_0$  or an equatorward MSE transport (green and black line respectively in Fig. 11d), illustrating that a double ITCZ in precipitation is not necessarily associated with an equatorward MSE flux at low latitudes. Instead a negative  $[AEI]_0$  is a sufficient but not a necessary condition for a double ITCZ in precipitation. Because of local energy conservation issues, which are discussed further in section 4, it is challenging to understand F1.13PC0.57, which shows a negative  $[AEI]_0$  and a positive equatorial  $\partial_y[\widehat{v\bar{h}}]$  (Fig. 11b) [contradicting Eq. (1) as steady state has been reached].

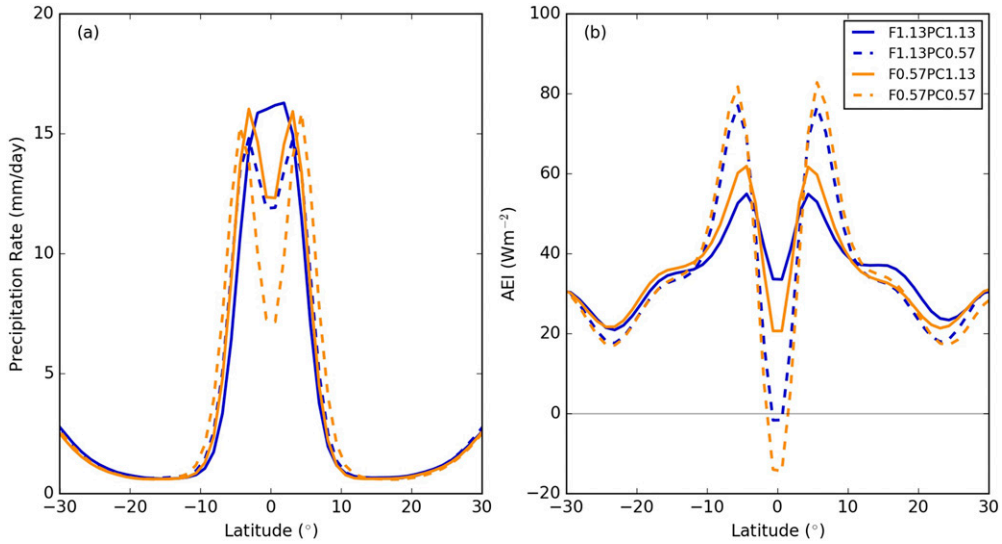


FIG. 10. Zonal-mean, time-mean (a) precipitation rates ( $\text{mm day}^{-1}$ ) and (b) AEI ( $\text{W m}^{-2}$ ) in simulations with a prescribed CRE.

4. Discussion

We have analyzed aquaplanet simulations with variations to convective mixing to show an association

between resultant variations in the AEI and characteristics of the ITCZ. Using the AEI framework we have shown the importance of the CRE in the sensitivity of the ITCZ to convective mixing. In a single ITCZ

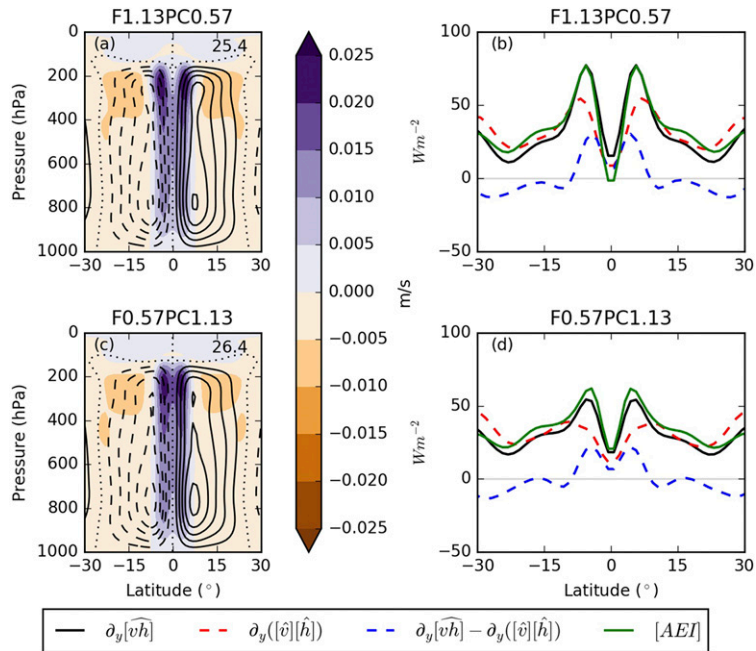


FIG. 11. (left) Zonal-mean, time-mean mass meridional streamfunction ( $\text{kg s}^{-1}$ ) (lined contours) and vertical wind speed ( $\text{m s}^{-1}$ ) (filled contours) for (a) F1.13PC0.57 and (c) F0.57PC1.13. Lined contours are in intervals of  $5 \times 10^{10}$ , with dashed contours representing negative values. Dotted contour is zero value and the maximum value of the mass meridional streamfunction is printed in top right-hand corner of each subplot. (right) Divergence of the MSE flux ( $\text{W m}^{-2}$ ) and AEI for (b) F1.13PC0.57 and (d) F0.57PC1.13. Solid black line indicates divergence of total MSE flux  $\partial_y[\widehat{v}\widehat{h}]$ , red dotted line is MSE flux due to mean circulation  $\partial_y[\widehat{v}][\widehat{h}]$ , blue line is  $\partial_y[\widehat{v}\widehat{h}] - \partial_y[\widehat{v}][\widehat{h}]$ , and green line is  $[AEI]$ .

scenario (F0.85, F1.13, and F1.70), the CRE is critical in maintaining a positive  $[AEI]_0$ . For example, the  $[AEI]_0$  would be negative without the CRE in F1.13 and F1.70, associated with a double ITCZ. Changes in cloudy-sky radiation are the dominant cause of AEI changes when varying the convective mixing rate, leading to our hypothesis that prescribing the CRE would remove or reduce the sensitivity of the ITCZ to convective mixing. The fact that the sensitivity of the ITCZ to  $f_{dp}$  remains in CRE-off and prescribed CRE simulations highlights the importance of other AEI components, in particular the latent heat flux. All simulations, with the exception of F0.57PC1.13, are consistent with [Bischoff and Schneider \(2016\)](#): a positive  $[AEI]_0$  is associated with a single ITCZ and a negative  $[AEI]_0$  with a double ITCZ.

CRE-off simulations illustrate that the CRE plays a substantial role in the structure and intensity of the ITCZ. Similar to [Harrop and Hartmann \(2016\)](#), we observe that removing the CRE cools the tropical upper troposphere, reducing atmospheric stability and resulting in deep convection over cooler SSTs. Stronger convection at higher latitudes reduces equatorial moisture convergence and is associated with a double ITCZ. Removing the CRE also weakens the Hadley circulation, which is associated with a reduced AEI gradient between the tropics and subtropics, in agreement with [Popp and Silvers \(2017\)](#). The sensitivity of the ITCZ to  $f_{dp}$  reduces when removing the CRE, agreeing with our hypothesis that prescribing the CRE would either remove or reduce the sensitivity of the ITCZ to convective mixing. Quantifying the reduction in sensitivity of the ITCZ to  $f_{dp}$  when removing the CRE remains a challenge due to strong dependence on the chosen metric and range of  $f_{dp}$ . It should also be noted that when removing the CRE other AEI components change, such that the AEI change is not equal to the total CRE that is removed.

In prescribed CRE simulations, ITCZ characteristics are sensitive to both the prescribed CRE and  $f_{dp}$ , however the sensitivity of the ITCZ to  $f_{dp}$  reduces by  $\approx 50\%$  ([Table 3](#)). In prescribed CRE simulations the response of convection to changes in convective mixing is offset by the effect of prescribing the location of the CRE. Heating associated with the prescribed CRE is a MSE source; therefore, to increase the MSE exported, convective activity increases. The reduction in sensitivity compliments work by [Voigt et al. \(2014\)](#), who found that prescribing the CRE reduced the sensitivity of the ITCZ to hemispheric albedo perturbations to a similar degree. Thus, the role of the CRE in the sensitivity of the ITCZ to both variations in the convection scheme and boundary forcing appear similar, based on these two studies.

In both CRE-off and prescribed CRE simulations, latent heat flux alterations, associated with circulation

changes, are the predominant cause of AEI changes when varying  $f_{dp}$ . Circulation changes when varying  $f_{dp}$  in CRE-off simulations are not associated with clear-sky flux variations, consistent with [Harrop and Hartmann \(2016\)](#), who concluded that changes in the clear-sky radiative cooling do not change the modeled circulation. [Mobis and Stevens \(2012\)](#) highlighted the importance of surface fluxes in reducing the sensitivity of the ITCZ to the convective parameterization scheme when prescribing the wind speeds in the computation of surface fluxes. [Numaguti \(1993\)](#) and [Liu et al. \(2010\)](#) also concluded that variations in surface evaporation are associated with the ITCZ structure. We highlight that the sensitivity of the ITCZ to convective mixing is predominantly associated with surface fluxes in the absence of cloud feedbacks.

As noted earlier in [sections 3c and 3d](#), the balance between the diagnosed AEI and diagnosed  $\partial_y[\overline{vh}]$ , Eq. (1), does not hold locally in MetUM. The mean of the maximum absolute diagnosed imbalance across the tropics amongst simulations is  $13.4 \text{ W m}^{-2}$ . More importantly, the diagnosed equatorial energy imbalance ranges from  $6.94 \text{ W m}^{-2}$  in F0.28NC to  $-20.63 \text{ W m}^{-2}$  in F1.70 with a mean absolute error of  $9.89 \text{ W m}^{-2}$ . For all of our simulations apart from F1.13PC0.57, the signs of the equatorial  $d_y[\overline{vh}]$  and  $[AEI]_0$  are the same, and therefore using  $[AEI]_0$  as a proxy for the direction of energy transport at low latitudes is still valid. In F1.13PC0.57 the difference between the diagnosed  $d_y[\overline{vh}]$  and  $[AEI]_0$  is  $-16.9 \text{ W m}^{-2}$ ; the equatorial  $d_y[\overline{vh}]$  is positive and  $[AEI]_0$  is slightly negative ([Fig. 11b](#)). While the local energy imbalance is a concern for F1.13PC0.57, we argue that in all other simulations the local energy imbalance does not affect our conclusions. There are a number of possible reasons for the localized imbalance of the AEI budget including non-conservation associated with the semi-Lagrangian advection scheme in MetUM; the use of dry and moist density in different components of the MetUM dynamics and physics, errors in our diagnosis of the MSE budget (e.g., not considering density changes within a time step), or using an Eulerian approach for diagnosing the energy transport, which is inconsistent with the semi-Lagrangian advection scheme. It is worth noting that other studies using the AEI framework have not shown that the MSE energy budget is locally closed, and this problem may not be unique to our study. Nevertheless, the local energy imbalance has challenged our interpretation of some simulations, and highlights that future modeling studies using an atmospheric MSE budget should be cautious.

Variations in the CRE when varying  $f_{dp}$  can lead to a negative  $[AEI]_0$  associated with a net equatorward MSE

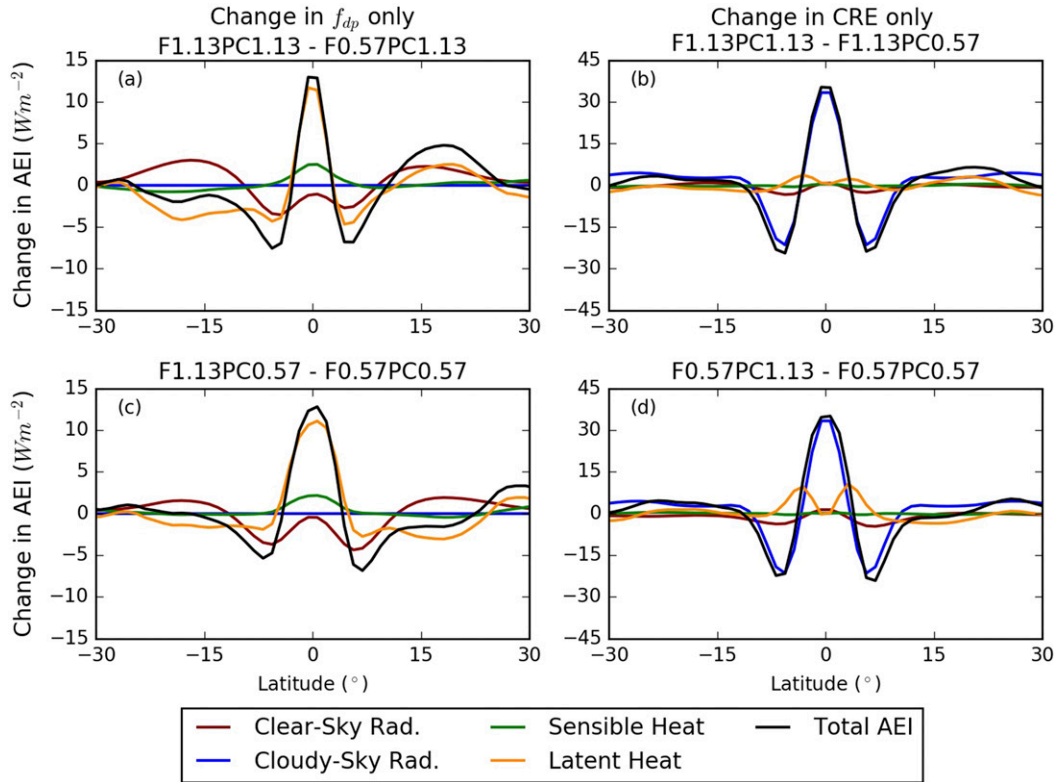


FIG. 12. Changes in zonal-mean, time-mean AEI contributions ( $\text{W m}^{-2}$ ) for prescribed-CRE simulations. (a),(c) Comparison of simulations with same  $f_{dp}$  constant with y-axis limits from  $-15$  to  $15 \text{ W m}^{-2}$ . (b),(d) Comparison of simulations with a different prescribed CRE with y-axis limits from  $-45$  to  $45 \text{ W m}^{-2}$ .

energy transport at low latitudes. While the predominant response to a negative  $[\text{AEI}]_0$  is a double ITCZ associated with equatorward energy transport at low latitudes by the mean circulation (F0.28, F0.28NC, and F0.57NC), F0.57, F0.85NC, and F1.13NC have shown that a net equatorward MSE transport can occur at low latitudes even with a poleward energy transport by the mean flow at the tropopause. Two mechanisms can lead to this. First, the MSE flux due to eddies contributes a substantial proportion to the total MSE flux (as seen in Figs. 11 and 12b,d), and this can support equatorward MSE transport. In F0.57, the MSE flux due to eddies is responsible for a net equatorward energy transport in the deep tropics. This invalidates the assumption that the energy flux equator is associated with zero MSE

transport by the mean circulation, as in Bischoff and Schneider (2016). This is also supported by the equatorward displacement of the energy flux equator [(from Eqs. (2) and (4)] relative to maximum precipitation in all simulations except for F0.85NC and F1.70NC (Table 4). The second mechanism (F0.85NC and F1.13NC) is a change in the MSE transport direction due to a shallower Hadley circulation and a lower MSE in the upper-troposphere (section 3c). These changes reduce the MSE export in the upper branch of the Hadley circulation, resulting in an equatorward MSE transport by the mean circulation at low latitudes.

In our aquaplanet configuration SSTs are fixed which implies an arbitrary but varying oceanic heat transport to maintain SSTs given a net surface heat flux

TABLE 3. Root-mean-square difference for tropical precipitation and mass meridional streamfunction between two simulations. Tropical domain defined as  $30^\circ\text{N}$  to  $30^\circ\text{S}$ . Percentage value is the percentage reduction compared to F0.57 and F1.13.

Simulations	Precipitation ( $\text{mm day}^{-1}$ )	Mass meridional streamfunction ( $\times 10^{10} \text{ kg s}^{-1}$ )
F0.57 and F1.13	2.84	1.78
F0.57PC1.13 and F1.13PC1.13	1.18 (58%)	0.67 (62%)
F0.57PC0.57 and F1.13PC0.57	1.65 (42%)	0.96 (46%)

TABLE 4.  $AEI_0$ , location of ITCZ, and approximate energy flux equator ( $\delta$ ) using Eqs. (2) or (4) in each simulation. A single (double) ITCZ is assumed when  $AEI_0$  is positive (negative). Not applicable (N/A) occurs when  $AEI_0$  and  $\partial_{yy}([AEI])_0$  are both negative and therefore the square root of  $-6([AEI])_0/\partial_{yy}([AEI])_0$  has an imaginary component.

Simulation	$AEI_0$ ( $W m^{-2}$ )	ITCZ location ( $^{\circ}$ )	Energy flux equator ( $\delta$ ) location ( $^{\circ}$ )
F0.28	-18.1	8.13/-8.13	6.85/-7.06
F0.57	-5.9	4.38/-4.38	0.84/-2.87
F0.85	33.4	1.88	-0.41
F1.13	36.7	0.63	0.22
F1.70	33.7	0.63	0.30
F0.28NC	-4.9	9.38/-9.38	N/A
F0.57NC	-12.2	8.13/-8.13	N/A
F0.85NC	-18.3	6.88/-5.63	6.48/-6.80
F1.13NC	-5.9	4.38/-4.38	3.21/-3.58
F1.70NC	2.0	1.88	2.73
F1.13PC1.13	33.6	0.63	0.16
F1.13PC0.57	-1.7	3.13/-3.13	0.19/-1.75
F0.57PC1.13	20.6	3.13	-0.12
F0.57PC0.57	-14.2	4.38/-4.38	2.70/-2.64

imbalance. Thus, our aquaplanet experiments may be viewed as energetically inconsistent. In Bischoff and Schneider (2014) and Voigt et al. (2016) ocean heat transport, and hence the net downward flux at the surface, is fixed, constraining the response of AEI components and potentially reducing the sensitivity of the ITCZ to model perturbations. In reality the ocean circulation, and thus ocean heat transport, is sensitive to changes in the surface wind stress. Therefore, both the SST and ocean heat transport could change in response to tropical circulation changes from variations to  $f_{dp}$  or the prescribed CRE. Recent work has shown that the ocean circulation plays an important role in the meridional transport of energy (Green and Marshall 2017), and that sensitivities of the ITCZ found in atmosphere-only simulations do not necessarily hold in a fully coupled model. For example, coupling reduces the sensitivity of the ITCZ to an interhemispheric albedo forcing [e.g., comparing Kay et al. (2016) and Hawcroft et al. (2017) to Voigt et al. (2014)]. The radiative effect of clouds on the surface and Ekman heat transport associated with a single ITCZ would be expected to reduce the equatorial SST gradient, which would promote a double ITCZ (Numaguti 1995; Mobis and Stevens 2012) and may reduce the sensitivity of the ITCZ to convective mixing. Coupled simulations with an interactive ocean are required to further investigate the sensitivity of the ITCZ to the CRE and convective mixing.

## 5. Conclusions

The double ITCZ bias is a leading systematic error across a hierarchy of models (Li and Xie 2014; Oueslati and Bellon 2015). Intermodel variability in the ITCZ

structure persists even in a highly idealized framework such as an aquaplanet with prescribed SSTs (Blackburn et al. 2013). This study confirms and extends previous research that variations in the convective parameterization scheme and convective mixing can alter the ITCZ (Fig. 1a; Hess et al. 1993; Numaguti 1995; Chao and Chen 2004; Liu et al. 2010; Mobis and Stevens 2012). Higher convective mixing rates are associated with a single ITCZ while lower rates are associated with a double ITCZ. As the convective mixing rate reduces, convection at higher latitudes strengthens, decreasing equatorward low-level winds at low latitudes, promoting a double ITCZ structure. The sensitivity of the ITCZ to convective mixing is associated with AEI changes, predominantly caused by CRE variations. For example, the CRE plays an important role in maintaining a positive equatorial AEI, and is therefore associated with a single ITCZ structure [consistent with Harrop and Hartmann (2016) and Bischoff and Schneider (2016)'s framework]. When removing the CRE, the response of the ITCZ depends on the convective mixing rate. At low convective mixing rates, where a double ITCZ is simulated with the CRE, precipitation bands shift poleward. At high convective mixing rates the ITCZ broadens, while at certain convective mixing rates the ITCZ structure changes from single to double. Quantifying whether the sensitivity of the ITCZ to convective mixing reduces when removing the CRE is challenging, as the sensitivity depends on the range of convective mixing rates and the chosen metric. Prescribing the CRE reduces the sensitivity of the ITCZ to convective mixing by  $\approx 50\%$ . When removing or prescribing the CRE other AEI components, in particular the latent heat flux, play a role in the sensitivity of the ITCZ to convective mixing. Hence, simulations where the ocean heat transport is fixed, thereby constraining surface fluxes, may underestimate the sensitivity



of the ITCZ to changes in model formulation. We have also shown two mechanisms responsible for a net equatorward MSE transport even with no equatorial subsidence: MSE transport by eddies, and a reduced MSE export in the upper branch of the mean circulation due to a shallower Hadley circulation. These mechanisms highlight that caution should be taken when associating changes in the AEI to the ITCZ structure.

**Acknowledgments.** JT is funded by the Natural Environment Research Council (NERC) via the SCENARIO Doctoral Training Partnership (NE/L002566/1) at the University of Reading. SJW was supported by the National Centre for Atmospheric Science, a NERC collaborative centre under Contract R8/H12/83/001. NPK was supported by an Independent Research Fellowship from the NERC (NE/LO10976/1). The data used in this publication are available on request from the lead author. We thank Aiko Voigt and two anonymous reviewers for comments that substantially improved this paper.

#### REFERENCES

- Adam, O., T. Bischoff, and T. Schneider, 2016: Seasonal and interannual variations of the energy flux equator and ITCZ. Part I: Zonally averaged ITCZ position. *J. Climate*, **29**, 3219–3230, <https://doi.org/10.1175/JCLI-D-15-0512.1>.
- Allan, R. P., 2011: Combining satellite data and models to estimate cloud radiative effect at the surface and in the atmosphere. *Meteor. Appl.*, **18**, 324–333, <https://doi.org/10.1002/met.285>.
- Bischoff, T., and T. Schneider, 2014: Energetic constraints on the position of the intertropical convergence zone. *J. Climate*, **27**, 4937–4951, <https://doi.org/10.1175/JCLI-D-13-00650.1>.
- , and —, 2016: The equatorial energy balance, ITCZ position, and double-ITCZ bifurcations. *J. Climate*, **29**, 2997–3013, <https://doi.org/10.1175/JCLI-D-15-0328.1>; Corrigendum, **29**, 7167–7167, <https://doi.org/10.1175/JCLI-D-16-0514.1>.
- Blackburn, M., and Coauthors, 2013: The aqua-planet experiment (APE): Control SST simulation. *J. Meteor. Soc. Japan*, **91A**, 17–56, <https://doi.org/10.2151/jmsj.2013-A02>.
- Bush, S., A. Turner, S. Woolnough, G. Martin, and N. Klingaman, 2015: The effect of increased convective entrainment on Asian monsoon biases in the MetUM general circulation model. *Quart. J. Roy. Meteor. Soc.*, **141**, 311–326, <https://doi.org/10.1002/qj.2371>.
- Chao, W. C., and B. Chen, 2004: Single and double ITCZ in an aqua-planet model with constant sea surface temperature and solar angle. *Climate Dyn.*, **22**, 447–459, <https://doi.org/10.1007/s00382-003-0387-4>.
- Chikira, M., 2010: A cumulus parameterization with state-dependent entrainment rate. Part II: Impact on climatology in a general circulation model. *J. Atmos. Sci.*, **67**, 2194–2211, <https://doi.org/10.1175/2010JAS3317.1>.
- Crueger, T., and B. Stevens, 2015: The effect of atmospheric radiative heating by clouds on the Madden–Julian oscillation. *J. Adv. Model. Earth Syst.*, **7**, 854–864, <https://doi.org/10.1002/2015MS000434>.
- Derbyshire, S. H., I. Beau, P. Bechtold, J.-Y. Grandpeix, J.-M. Piriou, J.-L. Redelsperger, and P. M. M. Soares, 2004: Sensitivity of moist convection to environmental humidity. *Quart. J. Roy. Meteor. Soc.*, **130**, 3055–3079, <https://doi.org/10.1256/qj.03.130>.
- Donohoe, A., J. Marshall, D. Ferreira, and D. Mcgee, 2013: The relationship between ITCZ location and cross-equatorial atmospheric heat transport: From the seasonal cycle to the Last Glacial Maximum. *J. Climate*, **26**, 3597–3618, <https://doi.org/10.1175/JCLI-D-12-00467.1>.
- Fermepin, S., and S. Bony, 2014: Influence of low-cloud radiative effects on tropical circulation and precipitation. *J. Adv. Model. Earth Syst.*, **6**, 513–526, <https://doi.org/10.1002/2013MS000288>.
- Frierson, D. M. W., 2007: The dynamics of idealized convection schemes and their effect on the zonally averaged tropical circulation. *J. Atmos. Sci.*, **64**, 1959–1976, <https://doi.org/10.1175/JAS3935.1>.
- , and Y. Hwang, 2012: Extratropical influence on ITCZ shifts in slab ocean simulations of global warming. *J. Climate*, **25**, 720–733, <https://doi.org/10.1175/JCLI-D-11-00116.1>.
- Fritsch, J. M., and C. F. Chappell, 1980: Numerical prediction of convectively driven mesoscale pressure systems. Part I: Convective parameterization. *J. Atmos. Sci.*, **37**, 1722–1733, [https://doi.org/10.1175/1520-0469\(1980\)037<1722:NPOCDM>2.0.CO;2](https://doi.org/10.1175/1520-0469(1980)037<1722:NPOCDM>2.0.CO;2).
- Green, B., and J. Marshall, 2017: Coupling of trade winds with ocean circulation damps ITCZ shifts. *J. Climate*, **30**, 4395–4411, <https://doi.org/10.1175/JCLI-D-16-0818.1>.
- Gregory, D., and P. Rowntree, 1990: A mass flux convection scheme with representation of cloud ensemble characteristics and stability-dependent closure. *Mon. Wea. Rev.*, **118**, 1483–1506, [https://doi.org/10.1175/1520-0493\(1990\)118<1483:AMFCSW>2.0.CO;2](https://doi.org/10.1175/1520-0493(1990)118<1483:AMFCSW>2.0.CO;2).
- Harrop, B., and D. Hartmann, 2016: The role of cloud radiative heating in determining the location of the ITCZ in aquaplanet simulations. *J. Climate*, **29**, 2714–2763, <https://doi.org/10.1175/JCLI-D-15-0521.1>.
- Hawcroft, M., J. M. Haywood, M. Collins, A. Jones, A. C. Jones, and G. Stephens, 2017: Southern Ocean albedo, inter-hemispheric energy transports and the double ITCZ: Global impacts of biases in a coupled model. *Climate Dyn.*, **48**, 2279–2295, <https://doi.org/10.1007/s00382-016-3205-5>.
- Hess, P. G., D. S. Battisti, and P. J. Rasch, 1993: Maintenance of the intertropical convergence zones and the large-scale tropical circulation on a water-covered Earth. *J. Atmos. Sci.*, **50**, 691–713, [https://doi.org/10.1175/1520-0469\(1993\)050<0691:MOTICZ>2.0.CO;2](https://doi.org/10.1175/1520-0469(1993)050<0691:MOTICZ>2.0.CO;2).
- Kang, S., I. Held, D. Frierson, and Z. Ming, 2008: The response of the ITCZ to extratropical thermal forcing: Idealized slab-ocean experiments with a GCM. *J. Climate*, **21**, 3521–3532, <https://doi.org/10.1175/2007JCLI2146.1>.
- Kay, J. E., C. Wall, V. Yettella, B. Medeiros, C. Hannay, P. Caldwell, and C. Bitz, 2016: Global climate impacts of fixing the Southern Ocean shortwave radiation bias in the Community Earth System Model (CESM). *J. Climate*, **29**, 4617–4636, <https://doi.org/10.1175/JCLI-D-15-0358.1>.
- Li, G., and S.-P. Xie, 2014: Tropical biases in CMIP5 multimodel ensemble: The excessive equatorial Pacific cold tongue and double ITCZ problems. *J. Climate*, **27**, 1765–1780, <https://doi.org/10.1175/JCLI-D-13-00337.1>.
- Li, Y., D. W. J. Thompson, and S. Bony, 2015: The influence of atmospheric cloud radiative effects on the large-scale atmospheric circulation. *J. Climate*, **28**, 7263–7278, <https://doi.org/10.1175/JCLI-D-14-00825.1>.
- Lin, J., 2007: The double-ITCZ problem in IPCC AR4 coupled GCMs: Ocean–atmosphere feedback analysis. *J. Climate*, **20**, 4497–4525, <https://doi.org/10.1175/JCLI4272.1>.
- Liu, Y., L. Guo, G. Wu, and Z. Wang, 2010: Sensitivity of ITCZ configuration to cumulus convective parameterizations on an

- aqua planet. *Climate Dyn.*, **34**, 223–240, <https://doi.org/10.1007/s00382-009-0652-2>.
- Mobis, B., and B. Stevens, 2012: Factors controlling the position of the Intertropical Convergence Zone on an aquaplanet. *J. Adv. Model. Earth Syst.*, **4**, M00A04, <https://doi.org/10.1029/2012MS000199>.
- Neale, R., and B. Hoskins, 2001: A standard test for AGCMs including their physical parametrizations: I: The proposal. *Atmos. Sci. Lett.*, **1**, 101–107, <https://doi.org/10.1006/asle.2000.0022>.
- Neelin, J. D., and I. M. Held, 1987: Modeling tropical convergence based on the moist static energy budget. *Mon. Wea. Rev.*, **115**, 3–12, [https://doi.org/10.1175/1520-0493\(1987\)115<0003:MTCBOT>2.0.CO;2](https://doi.org/10.1175/1520-0493(1987)115<0003:MTCBOT>2.0.CO;2).
- Nolan, D., S. Tulich, and J. Blanco, 2016: ITCZ structure as determined by parameterized versus explicit convection in aquachannel and aquapatch simulations. *J. Adv. Model. Earth Syst.*, **8**, 425–452, <https://doi.org/10.1002/2015MS000560>.
- Nordeng, T. E., 1994: Extended versions of the convective parametrization scheme at ECMWF and their impact on the mean and transient activity of the model in the tropics. ECMWF Tech. Memo. 206, 41 pp., <https://www.ecmwf.int/en/elibrary/11393-extended-versions-convective-parametrization-scheme-ecmwf-and-their-impact-mean>.
- Numaguti, A., 1993: Dynamics and energy balance of the Hadley circulation and the tropical precipitation zones: Significance of the distribution of evaporation. *J. Atmos. Sci.*, **50**, 1874–1887, [https://doi.org/10.1175/1520-0469\(1993\)050<1874:DAEBOT>2.0.CO;2](https://doi.org/10.1175/1520-0469(1993)050<1874:DAEBOT>2.0.CO;2).
- , 1995: Dynamics and energy balance of the Hadley circulation and the tropical precipitation zones. Part II: Sensitivity to meridional SST distribution. *J. Atmos. Sci.*, **52**, 1128–1141, [https://doi.org/10.1175/1520-0469\(1995\)052<1128:DAEBOT>2.0.CO;2](https://doi.org/10.1175/1520-0469(1995)052<1128:DAEBOT>2.0.CO;2).
- Oueslati, B., and G. Bellon, 2013: Convective entrainment and large-scale organization of tropical precipitation: Sensitivity of the CNRM-CM5 hierarchy of models. *J. Climate*, **26**, 2931–2946, <https://doi.org/10.1175/JCLI-D-12-00314.1>.
- , and —, 2015: The double ITCZ bias in CMIP5 models: Interaction between SST, large-scale circulation and precipitation. *Climate Dyn.*, **44**, 585–607, <https://doi.org/10.1007/s00382-015-2468-6>.
- Popp, M., and L. G. Silvers, 2017: Double and single ITCZs with and without clouds. *J. Climate*, **30**, 9147–9166, <https://doi.org/10.1175/JCLI-D-17-0062.1>.
- Schneider, T., T. Bischoff, and G. Haug, 2014: Migrations and dynamics of the intertropical convergence zone. *Nature*, **513**, 45–53, <https://doi.org/10.1038/nature13636>.
- Slingo, A., and J. M. Slingo, 1988: The response of a general circulation model to cloud longwave radiative forcing. I: Introduction and initial experiments. *Quart. J. Roy. Meteor. Soc.*, **114**, 1027–1062, <https://doi.org/10.1002/qj.49711448209>.
- Sobel, A. H., J. Nilsson, and L. M. Polvani, 2001: The weak temperature gradient approximation and balanced tropical moisture waves. *J. Atmos. Sci.*, **58**, 3650–3665, [https://doi.org/10.1175/1520-0469\(2001\)058<3650:TWTGAA>2.0.CO;2](https://doi.org/10.1175/1520-0469(2001)058<3650:TWTGAA>2.0.CO;2).
- Terray, L., 1998: Sensitivity of climate drift to atmospheric physical parameterizations in a coupled ocean–atmosphere general circulation model. *J. Climate*, **11**, 1633–1658, [https://doi.org/10.1175/1520-0442\(1998\)011<1633:SOCDTA>2.0.CO;2](https://doi.org/10.1175/1520-0442(1998)011<1633:SOCDTA>2.0.CO;2).
- Tiedtke, M., 1989: A comprehensive mass flux scheme for cumulus parameterization in large-scale models. *Mon. Wea. Rev.*, **117**, 1779–1800, [https://doi.org/10.1175/1520-0493\(1989\)117<1779:ACMFSF>2.0.CO;2](https://doi.org/10.1175/1520-0493(1989)117<1779:ACMFSF>2.0.CO;2).
- Voigt, A., S. Bony, J.-L. Dufresne, and B. Stevens, 2014: The radiative impact of clouds on the shift of the intertropical convergence zone. *Geophys. Res. Lett.*, **41**, 4308–4315, <https://doi.org/10.1002/2014GL060354>.
- , and Coauthors, 2016: The tropical rain belts with an annual cycle and a continent model intercomparison project: TRACMIP. *J. Adv. Model. Earth Syst.*, **8**, 1868–1891, <https://doi.org/10.1002/2016MS000748>.
- Walters, D., and Coauthors, 2017: The Met Office Unified Model Global Atmosphere 7.0/7.1 and JULES Global Land 7.0 configurations. *Geosci. Model Dev. Discuss.*, <https://doi.org/10.5194/gmd-2017-291>, in press.
- Wang, Y., L. Zhou, and K. Hamilton, 2007: Effect of convective entrainment/detrainment on the simulation of the tropical precipitation diurnal cycle. *Mon. Wea. Rev.*, **135**, 567–585, <https://doi.org/10.1175/MWR3308.1>.